A Parallel Comparison of Multiple Pairs of Images on Quantum Computers

Article *in* International Journal of Innovative Computing and Applications · July 2013

DOI: 10.1504/IJICA.2013.062955

6 authors, including:

Fei Yan
Changchun University of Science and Technology
49 PUBLICATIONS **386** CITATIONS
SEE PROFILE

Abdullah M. Iliyasu
Tokyo Institute of Technology
75 PUBLICATIONS **1,293** CITATIONS
SEE PROFILE

Fangyan Dong
Tokyo Institute of Technology
118 PUBLICATIONS **1,184** CITATIONS
SEE PROFILE

A parallel comparison of multiple pairs of images on quantum computers

Fei Yan*

Department of Computational Intelligence and Systems Science,
Tokyo Institute of Technology,
G3-49, 4259 Nagatsuta, Midori-ku,
Yokohama, 226-8502, Japan
E-mail: yan@hrt.dis.titech.ac.jp
*Corresponding author

Abdullah M. Iliyasu

Department of Computational Intelligence and Systems Science,
Tokyo Institute of Technology,
G3-49, 4259 Nagatsuta, Midori-ku,
Yokohama, 226-8502, Japan
and
College of Engineering,
Salman Bin Abdul-Aziz University,
P.O. Box 173, Al-Kharj 11942, Kingdom of Saudi Arabia
E-mail: iliyasu@hrt.dis.titech.ac.jp

Phuc Q. Le, Bo Sun, Fangyan Dong and Kaoru Hirota

Department of Computational Intelligence and Systems Science,
Tokyo Institute of Technology,
G3-49, 4259 Nagatsuta, Midori-ku,
Yokohama, 226-8502, Japan
E-mail: phuc@hrt.dis.titech.ac.jp
E-mail: sun@hrt.dis.titech.ac.jp
E-mail: tou@hrt.dis.titech.ac.jp
E-mail: hirota@hrt.dis.titech.ac.jp

Abstract: A method to compare multiple pairs of quantum images in parallel is proposed, where the similarities of the images are estimated according to the probability distributions of the readouts from quantum measurements. The proposed method by means of a single Hadamard gate with control-conditions to transform the entire information encoding the quantum images in a strip, offers a significant speed-up in comparison to performing the same task on traditional computing devices. Three simulation experiments comprising of the comparison of two images, multiple pairs of images, and the sub-blocks from two images are implemented using MATLAB to demonstrate the feasibility and efficiency of the parallel comparison. The proposal advances a fundamental step towards image searching on quantum computers in which the image with the highest similarity to a particular reference image is retrieved as a search result from a database.

Keywords: quantum computation; image processing; quantum image; quantum computer; quantum circuit; parallel comparison; similarity; probability distribution; image searching.

Reference to this paper should be made as follows: Yan, F., Iliyasu, A.M., Le, P.Q., Sun, B., Dong, F. and Hirota, K. (2013) 'A parallel comparison of multiple pairs of images on quantum computers', *Int. J. Innovative Computing and Applications*, Vol. 5, No. 4, pp.199–212.

Biographical notes: Fei Yan is a doctoral student at the Department of Computational Intelligence and Systems Science, Tokyo Institute of Technology, Japan. He obtained his BE in Computer Science and ME in Computer Networking and Communication from Changchun University of Science and Technology, China. His main research interests include quantum computation, quantum image processing, intelligent robotics, and data mining. In the past two years, he has been involved in several projects sponsored by the Japanese Government.

Abdullah M. Iliyasu obtained his ME and Doctor of Engineering degrees in Computational Intelligence and Intelligent Systems Science from the prestigious Tokyo Institute of Technology Japan, where he specialised in computational intelligence, quantum computation and quantum image processing. His other research interests include image processing, artificial intelligence, information security, cryptography, medical image processing, bio-informatics, fault-tolerant computing, robotics, and general topics in quantum-inspired computational intelligence, pattern recognition, and computer vision. An adept researcher, within the past two years he has co-authored more than two dozen publications in highly rated journals and proceedings of very reputable conferences. He is a listee in the *Marquis Who's Who in the World 2013*.

Phuc Q. Le is a special Postdoctoral Researcher at the Department of Computational Intelligence and Systems Science, Tokyo Institute of Technology, Japan from where he obtained both his ME and PhD with specialisation in computational intelligence, image processing, and quantum computation. His other research interests include machine learning, data mining, quantum cryptography, and computer programming.

Bo Sun is a doctoral student at the Department of Computational Intelligence and Systems Science, Tokyo Institute of Technology, Japan. He obtained his Bachelor of Engineering in Electrical Engineering and ME in Communication Engineering from Changchun University of Science and Technology, China. His main research interests include quantum computation, quantum image processing and pattern recognition.

Fangyan Dong received her PhD from the Department of Computational Intelligence and Systems Science, Tokyo Institute of Technology, Japan where she is working as an Assistant Professor. Her research interests include computational intelligence, logistics optimisation, kansei engineering, and intelligent robotics. She is a member of the Japan Society for Fuzzy Theory and Intelligent Informatics, Japanese Society for Artificial Intelligence, and Information Processing Society of Japan.

Kaoru Hirota received his BE, ME and Doctoral Engineering degrees from Tokyo Institute of Technology, Japan where he is currently a Professor. Before then, he was a Professor at Hosei University, Japan. He is a recipient of the Banki Donat and Henri Coanda medals, the Grigore MOISIL Award, and an Honorary Professorship from De La Salle University. He organised numerous international conferences/symposiums and he has published more than 150 journal papers and 350 conference papers. His research interests include computational intelligence, fuzzy systems, intelligent robotics, expert systems and multimedia intelligent communication among others.

1 Introduction

Quantum computation is a promising and rapidly growing field (Shor, 1994; Grover, 1996; Venegas-Andraca and Bose, 2003; Chow et al., 2012) that has witnessed a series of significant breakthroughs in the last decade. The current paradigm for implementing quantum algorithms is the quantum circuit model (Nielsen and Chuang, 2000), in which the algorithms are compiled into a sequence of simple gates acting on one or more qubits. Many of these quantum algorithms are expressed in terms of uniform special-purpose circuits that depend strongly on the problem at hand. These circuits comprise various levels of abstraction and combinations of the universal gates: NOT, Hadamard, controlled-NOT, and Toffoli gates. These gates combine to form what is often referred to in the literature as the NCT library (Iliyasu et al., 2011; Barenco et al., 1995).

Research on quantum image processing started with proposals on quantum image representations such as qubit lattice (Venegas-Andraca and Bose, 2003), real Ket (Latorre, 2005), and the flexible representation of quantum image (FRQI) (Le et al., 2010a, 2011c). By applying the elementary gates such as Pauli-X and Hadamard gates combined with appropriate quantum measurements (Childs et al., 2010) on these representations, some image processing operations can be executed. For example, several processing transformations have been proposed based on the FRQI representation among them are the geometric transformations, geometric transformations on quantum images (GTQI) (Le et al., 2010b) and the CTQI (Le et al., 2011a) that are focused on the colour information of the images. Moreover, applications such as a scheme to watermark and authenticate quantum images (Iliyasu et al., 2012a, 2012b) and a framework to produce movies on quantum computers (Iliyasu et al., 2011), have also been suggested based on the FRQI representation for the images.

Most of the operations on FRQI quantum images (Le et al., 2010b, 2011a; Iliyasu et al., 2012a), however, are focused on single images. This paper presents an attempt to extend this in order to compare multiple pairs of FRQI quantum images encoded in parallel. Succinctly put, the main contributions of this work include the following:

- Proposing a scheme for the parallel comparison of images on quantum computers.

- Ascertaining the relationship between the similarity of two quantum images and the probability of their post-measurement states.
- Analysing the similarities of multiple pairs of images and the sub-blocks from two images in parallel.

The comparison process is executed using low computational requirements, and hence, offers a significant speed-up in comparison with performing the same task on traditional computing devices, since only a single Hadamard gate as well as several control-conditions (when sub-blocks of two images are compared) could transform the entire information encoding the quantum images in a strip, simultaneously.

The quantum image processing framework for the FRQI, GTQI, and strip are reviewed in Section 2. The parallel comparison of multiple pairs of quantum images is analysed in Section 3. Three simulation experiments for different cases of image comparison are presented in Section 4.

2 Quantum image processing framework for FRQI, GTQI, and strip

The realisation of most quantum image processing applications will undoubtedly rely on using their corresponding classical operations as reference. In this section, a flexible representation for quantum images, FRQI, which is similar to the pixel representation for images on conventional computers is introduced initially, in addition, the geometric transformation based on FRQI which can swap two points, even two sub-blocks in an image is reviewed in Section 2.2. Ultimately, the strip comprising of 2^m quantum images is presented for the quantum image parallel comparison.

2.1 Flexible representation for quantum images

The flexible representation for quantum images, FRQI (Le et al., 2010a, 2011c), captures the essential information about the colours as well as the corresponding positions of every point in an image and integrates them into a quantum state having its formula in (1),

$$|I(n)\rangle = \frac{1}{2^n}\sum_{i=0}^{2^{2n}-1}|c_i\rangle \otimes |i\rangle, \tag{1}$$

where

$$|c_i\rangle = \cos\theta_i|0\rangle + \sin\theta_i|1\rangle, \tag{2}$$

$$\theta_i \in [0, \pi/2], i = 0, 1, \cdots, 2^{2n}-1, \tag{3}$$

where $|0\rangle$ and $|1\rangle$ are 2D computational basis quantum states, $|i\rangle$, $i = 0, 1, \cdots, 2^{2n} - 1$ are $2n$-D computational basis quantum states and $\theta = (\theta_0, \theta_1, \cdots, \theta_{2^{2n}-1})$, is the vector of angles encoding colours. There are two parts in the FRQI representation of an image; $|c_i\rangle$ and $|i\rangle$ which encode information about the colours and corresponding positions in the image, respectively. An example of a 2 × 2 FRQI quantum image is shown in Figure 1.

Figure 1 A 2 × 2 FRQI quantum image, its circuit structure and FRQI state

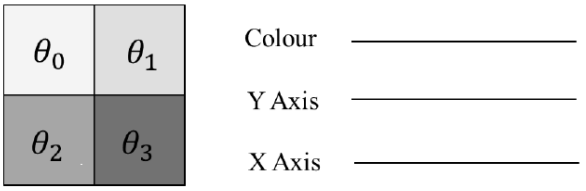

$$|I(1)\rangle = \frac{1}{2}[(\cos\theta_0|0\rangle + \sin\theta_0|1\rangle) \otimes |00\rangle + (\cos\theta_1|0\rangle + \sin\theta_1|1\rangle) \otimes |01\rangle + (\cos\theta_2|0\rangle + \sin\theta_2|1\rangle) \otimes |10\rangle + (\cos\theta_3|0\rangle + \sin\theta_3|1\rangle) \otimes |11\rangle]$$

2.2 General framework for GTQI

GTQI (Le et al., 2010b) are the operations which focus on manipulating the geometric information of the FRQI images, i.e., information about position of every point in the image. These transformations are akin to 'shuffling' the image content point-by-point. The global effect being a transformation of the original image to a new state whose nature is determined by the gate sequence of the operation needed to accomplish the desired transformation (Iliyasu et al., 2012a). Such transformations are referred to as geometric transformations, G_I, which on FRQI quantum images can be defined as in (4),

$$G_I\left(|I(n)\rangle\right) = \frac{1}{2^n}\sum_{i=0}^{2^{2n}-1}|c_i\rangle \otimes G(|i\rangle), \tag{4}$$

where $|I(n)\rangle$ is of the form defined in (1) and $G(|i\rangle)$ for $i = 0, 1, \ldots, 2^{2n}-1$ is the unitary transformation performing geometric exchanges based on the vertical and horizontal information represented by $|i\rangle$. The general structure of circuits for geometric transformations on FRQI images is shown in Figure 2.

Figure 2 Generalised circuit design for GTQI

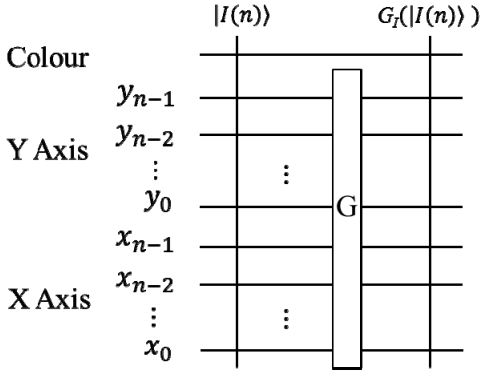

Using the GTQI operations, classical-like transformations such as flipping, swapping, or rotating an image can be performed on quantum computers using images encoded in the FRQI representation. The complexity of two-point swapping operation on n-sized FRQI images ($n \geq 2$) is $O(n^2)$ (Le et al., 2010b). Based on this, restricted geometric transformations on FRQI quantum images were proposed in

(Le et al., 2011b) in order to constrain the desired geometric transformation to a smaller sub-block of the image by imposing additional restrictions to indicate specific locations. The more the number of controls the transformations have, the less the size of the affected areas. Specifying the area in which the transformation will be applied increases the complexity of the new transformation in terms of the depth and the number of basic gates in the corresponding circuit.

2.3 Representation of strip encoding multiple FRQI images

A dextrous property of the strip representation (Iliyasu et al., 2011) to encode 2^m-ending FRQI images lies in its ability to utilise the parallelism inherent to quantum computation in order to transform multiple images using very few quantum resources. The definition of the strip and its properties are introduced in this section.

Definition 1: A strip, $|S(m, n)\rangle$, is an array comprising 2^m FRQI images, which is defined by

$$\left|S(m,n)\right\rangle = \frac{1}{2^{m/2}}\sum_{s=0}^{2^m-1}\left|I_s(n)\right\rangle \otimes |s\rangle, \tag{5}$$

where

$$\left|I_s(n)\right\rangle = \frac{1}{2^n}\sum_{i=0}^{2^{2n}-1}\left|c_{s,i}\right\rangle \otimes |i\rangle, \tag{6}$$

$$\left|c_{s,i}\right\rangle = \cos\theta_{s,i}|0\rangle + \sin\theta_{s,i}|1\rangle, \tag{7}$$

$$\theta_{s,i} \in \left[0, \frac{\pi}{2}\right], i = 0, 1, \cdots, 2^{2n}-1, s = 0, 1, \cdots, 2^m-1, \tag{8}$$

$|s\rangle$ is the position of each image in the strip, m is the number of qubits required to encode the images being compared, $|I_s(n)\rangle$ is a FRQI image as defined in (1) at position $|s\rangle$, $|c_{s,i}\rangle$ and $|i\rangle$ encode the information about the colours and their corresponding positions in the image $|I_s(n)\rangle$. The state $|S(m, n)\rangle$ is normalised, which can be confirmed by

$$\begin{aligned}\left\|\left|S(m,n)\right\rangle\right\| &= \frac{1}{2^{m/2}}\sqrt{\sum_{s=0}^{2^m-1}\left\|\left|I_s(n)\right\rangle\right\|^2} \\ &= \frac{1}{2^{m/2+n}}\sqrt{\sum_{s=0}^{2^m-1}\sum_{i=0}^{2^{2n}-1}\left(\cos^2\theta_{s,i}+\sin^2\theta_{s,i}\right)} = 1.\end{aligned} \tag{9}$$

As seen in Figure 3, the size of a strip in the representation captures the input state of the strip comprising 2^m quantum images. Each image in the strip is an FRQI state while the combination of such states in the strip is best represented as a *multiple* FRQI or simply *m*FRQI state. The *m*FRQI state can represent 2^m quantum images using only $m + 2n + 1$ qubits since all of the images are of the same size in this strip.

The 2^m-ending FRQI quantum images encoded in a strip can be horizontally-oriented or vertically-oriented (Yan et al., 2012). The latter case, the vertically-oriented strip, is implied throughout the ensuing discussion. Control-conditions on strip wires could control the image which is being processed, combining with the control-conditions from the position $|y\rangle|x\rangle$ to the colour wire; every pixel in this strip can be accessed.

Figure 3 Circuit structure to encode the strip input

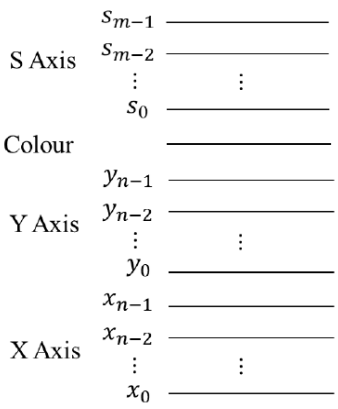

3 Parallel comparison of multiple pairs of quantum images

Inspired the importance of image searching and how it is accomplished on conventional computers, quantum image searching from a database appears to be an indispensable application in quantum image processing (Beach et al., 2003; Caraiman and Manta, 2009). It is envisaged that quantum image searching from a database will be faster than the classical ones because of the inherent parallelism of quantum computation (Moore and Nilsson, 2001; Broadbent and Kashefi, 2009). A first step towards realising that would be to propose a scheme to evaluate the extent to which two or more images are similar to one another. The main contribution of this paper is tailored towards achieving this essential step of quantum image searching. In the subsections that follow, we present the scheme to compare images in parallel on quantum computers, and the different cases in the comparison process such as the comparison of sub-blocks from two images.

3.1 Scheme to compare images in parallel on quantum computers

The scheme to compare quantum images on quantum computers, together with several momentous definitions as the basis of the ensuing discussions is presented in this section. It starts with the introduction of comparison for two quantum images. The comparison of two FRQI quantum images $|I_k(n)\rangle$ and $|I_t(n)\rangle$,

$$\left|I_k(n)\right\rangle = \frac{1}{2^n}\sum_{i=0}^{2^{2n}-1}\left(\cos\theta_{k,i}|0\rangle + \sin\theta_{k,i}|1\rangle\right)\otimes|i\rangle, \tag{10}$$

$$\left|I_t(n)\right\rangle = \frac{1}{2^n}\sum_{i=0}^{2^{2n}-1}\left(\cos\theta_{t,i}|0\rangle + \sin\theta_{t,i}|1\rangle\right)\otimes|i\rangle, \tag{11}$$

is that obtain the similarity, which is in the interval from 0 to 1, between them through the quantum operations. In addition, given a strip comprising 2^m quantum images, parallel comparison of quantum images retrieves the similarities between 2^{m-1} pairs of images in the strip simultaneously.

Definition 2: The difference between the i^{th} pixels of two FRQI images $|I_k(n)\rangle$ and $|I_t(n)\rangle$, as defined in (10) and (11), is given by

$$\sigma_{k,t}^{i} = \left|\theta_{k,i} - \theta_{t,i}\right|, \sigma_{k,t}^{i} \in [0, \pi/2], \tag{12}$$

where $\theta_{k,i}$ and $\theta_{t,i}$ represent the colour information at position i of the two images, respectively.

Definition 3: The similarity between two FRQI images $|I_k(n)\rangle$ and $|I_t(n)\rangle$, as defined in (10) and (11), is a function of pixel difference $\sigma_{k,t}$ at every position of the image given by

$$sim\left(\left|I_k\right\rangle, \left|I_t\right\rangle\right) = f\left(\sigma_{k,t}^{0}, \sigma_{k,t}^{1}, \cdots, \sigma_{k,t}^{2^{2n}-1}\right), \tag{13}$$

where $sim(|I_k\rangle, |I_t\rangle) \in [0, 1]$.

Two special cases of the similarity between two quantum images are listed as follows:

a *if* $\forall i,\ \sigma_{k,t}^{i} = \frac{\pi}{2}$, *then* $sim(|I_k\rangle, |I_t\rangle) = 0$ and the two images are totally different,

b *if* $\forall i,\ \sigma_{k,t}^{i} = 0$, *then* $sim(|I_k\rangle, |I_t\rangle) = 1$ and the two images are exactly the same,

where $i = 0,1, \ldots, 2^{2n} - 1$, $\sigma_{k,t}^{i}$ is the pixel difference at position i as defined in Definition 2.

Combining the properties of quantum computation, superposition and entanglement, the representation of strip which is introduced in Section 2.3 is supposed to be used for comparing quantum images of equal size because an operation on the strip wires can transform the information in all the images in the strip simultaneously. The strip does not only make the comparison of quantum images possible but it also provides an efficient way to compare multiple pairs of quantum images in parallel. The scheme to compare quantum images in parallel consists of three steps as detailed in Figure 4. These steps are outlined in this subsection.

Step 1 Preparation of the strip comprising 2^m quantum images

The quantum images are prepared into FRQI states using their classical versions images. The colour information as well as the corresponding positions of every point in the classical version is integrated into the quantum state, and 2^m quantum images being compared are combined to form a vertically-oriented strip. The routine involved in preparing FRQI quantum images and its extension to encode multiple FRQI images as a single register, called the strip, were discussed thoroughly in Le et al. (2010a), Iliyasu et al. (2011) and Yan et al. (2012). In all these instances, the availability of a classical version of each image from which the quantum versions of the images were prepared is implied.

Figure 4 Scheme to compare quantum images in parallel on quantum computers

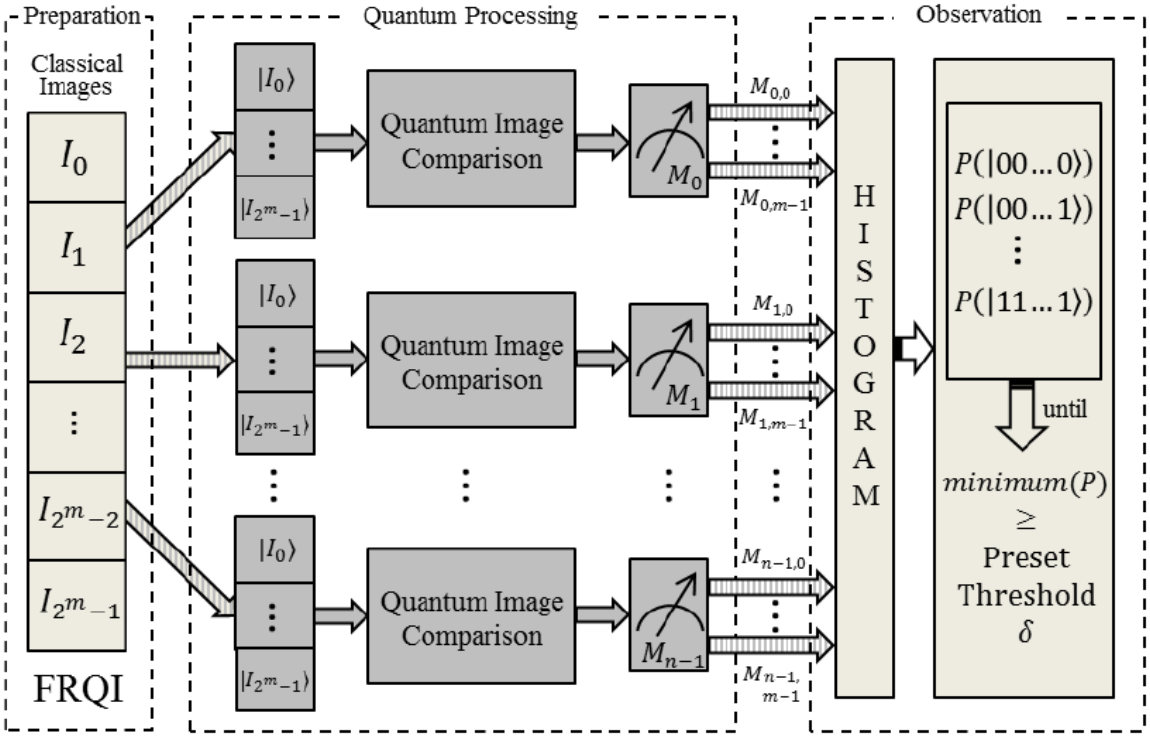

Step 2 Comparison of quantum images through quantum operations

The strip as prepared in the preceding period is transformed using a gate array comprising geometric, GTQI (Le et al., 2010b) and colour, CTQI, (Le et al., 2011a), transformations on all the images in the strip. For this particular application, the transformations are built in a way to allow the recovery of the pixel difference as defined in (12). This transformation step combines with measurement operations that follow it to convert the quantum information into the classical form as probability distributions. Since measurements are known to destroy the superposition state in quantum systems (Nielsen and Chuang, 2000), in order to compare the similarity between two FRQI quantum images (in parallel), the strip has to be prepared n (where $n > 1$) times.

Step 3 Observation of readouts from quantum measurements

The readouts from the n quantum measurements build up a histogram that implicitly reflects the probability distributions. Extracting and analysing these distributions gives information that the similarity values between the quantum images being compared. The strip preparation will be continued until $min(P(|s_{m-1}, \cdots, s_0\rangle)) \geq \delta$, where $min\left(P\left(|s_{m-1}, \cdots, s_0\rangle\right)\right)$ is the minimum of the probabilities of the readouts from the experiments, $\delta \in [0, 1]$ is a pre-set threshold, which can be read as the reasonable estimation for the similarity between two quantum images being compared.

The comparison of quantum images in this scheme is especially specified in the ensuing sections which are the evaluation of the similarity between two images, parallel comparison of multiple pairs of images, and the comparison of sub-blocks from two images.

3.2 Evaluation of the similarity between two quantum images

As the basis of discussing parallel quantum image comparison, the comparison between two quantum images should come first (Yan et al., 2012). According to (5), (10), and (11), the state of the strip comprising two images ($m = 1$, $k = 0$, $t = 1$, $s = 0, 1$) becomes

$$\left|S(1, n)\right\rangle = \frac{1}{\sqrt{2}}\left(\left|I_0(n)\right\rangle \otimes |0\rangle + \left|I_1(n)\right\rangle \otimes |1\rangle\right), \tag{14}$$

where

$$\left|I_0(n)\right\rangle = \frac{1}{2^n}\sum_{i=0}^{2^{2n}-1}\left(\cos\theta_{0,i}\,|0\rangle + \sin\theta_{0,i}\,|1\rangle\right)\otimes|i\rangle \tag{15}$$

and

$$\left|I_1(n)\right\rangle = \frac{1}{2^n}\sum_{i=0}^{2^{2n}-1}\left(\cos\theta_{1,i}\,|0\rangle + \sin\theta_{1,i}\,|1\rangle\right)\otimes|i\rangle \tag{16}$$

are the two FRQI quantum images being compared, which are located in the upper part and lower part of the strip, respectively.

The circuit structure to compare these two FRQI quantum images is shown in Figure 5. A Hadamard gate, $H = \frac{1}{\sqrt{2}}\begin{pmatrix}1 & 1\\ 1 & -1\end{pmatrix}$, which maps the basis state $|0\rangle$ to $(|0\rangle + |1\rangle)/\sqrt{2}$ and $|1\rangle$ to $(|0\rangle - |1\rangle)/\sqrt{2}$, , is applied on the strip wire s_0 to obtain the recombination of $|I_0(n)\rangle$ and $|I_1(n)\rangle$, it is then followed by a measurement operation M_0.

Figure 5 Generalised circuit structure for comparing two FRQI quantum images

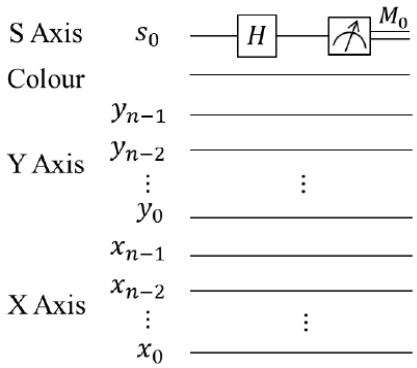

Corresponding to the circuit shown in Figure 5, the new state of the quantum system after applying the Hadamard gate on the strip wire s_0 (expressed by $H_0 \mid S(1, n)\rangle$) can be given as follows:

$$\begin{aligned} H_0\left|S(1, n)\right\rangle &= 1/\sqrt{2}\left(\left|I_0(n)\right\rangle \otimes H|0\rangle + \left|I_1(n)\right\rangle \otimes H|1\rangle\right)\\ &= 1/2\left[\left|I_0(n)\right\rangle \otimes \left(|0\rangle + |1\rangle\right) + \left|I_1(n)\right\rangle \otimes \left(|0\rangle - |1\rangle\right)\right]\\ &= 1/2\left[\left(\left|I_0(n)\right\rangle + \left|I_1(n)\right\rangle\right)\otimes|0\rangle + \left(\left|I_0(n)\right\rangle - \left|I_1(n)\right\rangle\right)\otimes|1\rangle\right], \end{aligned} \tag{17}$$

where

$$\begin{aligned} \left|I_0(n)\right\rangle \pm \left|I_1(n)\right\rangle = \frac{1}{2^n}\sum_{i=0}^{2^{2n-1}}\big[&\left(\cos\theta_{0,i} \pm \cos\theta_{1,i}\right)|0\rangle\\ &+\left(\sin\theta_{0,i} \pm \sin\theta_{1,i}\right)|1\rangle\big]|i\rangle. \end{aligned} \tag{18}$$

It is obvious that the result of the measurement M_0 depends on the disparities between $|I_0(n)\rangle$ and $|I_1(n)\rangle$. The state $|0\rangle$ and $|1\rangle$ exist on strip wire s_0 at a certain probability. In accordance with the measurement postulate in Nagy and Akl (2006), the probability of state $|0\rangle$ on this strip wire is

$$
\begin{aligned}
P_{s_0}(|0\rangle) &= \left(\frac{1}{2^{n+1}}\right)^2 \sum_{i=0}^{2^{2n}-1} \Big[\left(\cos\theta_{0,i} + \cos\theta_{1,i}\right)^2 \\
&\qquad + \left(\sin\theta_{0,i} + \sin\theta_{1,i}\right)^2 \Big] \\
&= \frac{1}{2^{2n+1}} \sum_{i=0}^{2^{2n}-1} \left[1 + \cos\left(\theta_{0,i} - \theta_{1,i}\right)\right] \\
&= \frac{1}{2} + \frac{1}{2^{2n+1}} \sum_{i=0}^{2^{2n}-1} \cos\sigma_{0,1}^{i}.
\end{aligned} \tag{19}
$$

In the same manner, that of state $|1\rangle$ on the same wire is

$$
P_{s_0}(|1\rangle) = \frac{1}{2} - \frac{1}{2^{2n+1}} \sum_{i=0}^{2^{2n}-1} \cos\sigma_{0,1}^{i}. \tag{20}
$$

The probabilities of these two states sum up to 1, i.e., $P_{s_0}(|0\rangle) + P_{s_0}(|1\rangle) = 1$, as they should.

It is apparent that, arising from (20) the pixel difference $\sigma_{0,1}^{i}$ is related to the probability of getting readout of 1 from the strip wire s_0, $P_{s_0}(|1\rangle)$, in the measurement and $P_{s_0}(|1\rangle)$ will increase when pixel difference increases. Furthermore, the similarity between two images, which is a function of the pixel differences at every position, depends on $P_{s_0}(|1\rangle)$ as given by

$$
sim\left(|I_0\rangle, |I_1\rangle\right) = 1 - 2P_{s_0}(|1\rangle) = \frac{1}{2^{2n}} \sum_{i=0}^{2^{2n}-1} \cos\sigma_{0,1}^{i}, \tag{21}
$$

where $|I_0\rangle$ and $|I_1\rangle$ are the two images being compared, $P_{s_0}(|1\rangle)$ is in the form defined in (20), and $sim(|I_0\rangle, |I_1\rangle) \in [0, 1]$. The similarity between $|I_0(n)\rangle$ and $|I_1(n)\rangle$ which are encoded in the strip is in line with the definition of similarity between two FRQI quantum images in (13), where

$$
f\left(\sigma_{k,t}^{0}, \sigma_{k,t}^{1}, \cdots, \sigma_{k,t}^{2^{2n}-1}\right) = \frac{1}{2^{2n}} \sum_{i=0}^{2^{2n}-1} \cos\sigma_{0,1}^{i}.
$$

Figure 6 Four strips where each comprises two images are considered in order to compare the four pairs of images

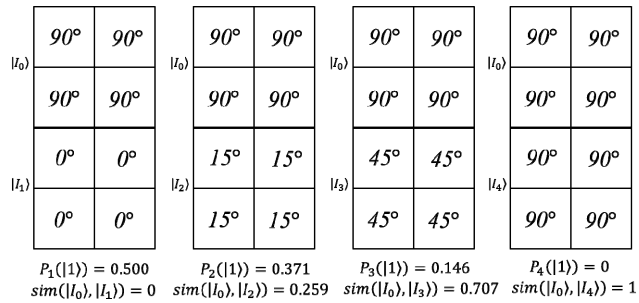

An example to compare the image $|I_0\rangle$ with $|I_1\rangle$, $|I_2\rangle$, $|I_3\rangle$, and $|I_4\rangle$ is presented in Figure 6. The probabilities of the readouts on strip wire s_0, $P_{s_0}(|1\rangle)$ in (20), from each pair of images are shown with $P_1(|1\rangle)$, $P_2(|1\rangle)$, $P_3(|1\rangle)$, and $P_4(|1\rangle)$ on the first row below the strip in the figure, and it is followed by the similarity value between the two images in the strip. It is trivial that $sim(|I_0\rangle, |I_1\rangle) < sim(|I_0\rangle, |I_2\rangle) < sim(|I_0\rangle, |I_3\rangle) < sim(|I_0\rangle, |I_4\rangle)$, actually, the images $|I_0\rangle$ and $|I_4\rangle$ have the same content.

3.3 A parallel comparison of multiple pairs of images in a strip

The parallel computation on quantum computer leads us to find a way that comparing many pairs of images in parallel. The proposal of the strip comprising 2^m images as defined in Definition 1 provides us a crucial condition to make it possible because the operation on the strip wires can transform the information in every image simultaneously. The generalised circuit structure of comparing 2^{m-1} pairs of quantum images in parallel is presented in Figure 7. By applying a Hadamard operation on the r^{th} strip wire in the circuit, s_r, the mathematical expressions between the two images being compared are realised. The final step in the procedure consists of m measurements from which the similarity can be retrieved in each pair of images.

Due to the representation of the strip and the property of Hadamard operation, only the specified pairs of images in the strip can be compared, which is the k^{th} image, $|I_k\rangle$, and the $(k + 2^r)^{\text{th}}$ image, $|I_{k+2^r}\rangle$ (r is the index of s_r in the circuit). Therefore, the mFRQI state of the strip when 2^{m-1} pairs of images are compared is

$$
\begin{aligned}
|S(m,n)\rangle &= \frac{1}{2^{m/2}} \sum_{s=0}^{2^m-1} |I_s(n)\rangle \otimes |s\rangle \\
&= \frac{1}{2^{m/2}} \sum_{z=1}^{2^{m-r-1}} \sum_{k=g(z)}^{\frac{1}{2}g(2z)-1} \left(|I_k\rangle \otimes |k\rangle + |I_{k+2^r}\rangle \otimes |k+2^r\rangle\right),
\end{aligned} \tag{22}
$$

$$
g(z) = (z-1)2^{r+1}, \tag{23}
$$

where $m \geq 2$, $|s\rangle = |s_{m-1}, \cdots, s_{r+1}, s_r, s_{r-1}, \cdots, s_0\rangle$, $s_r \in [0, 1]$.

Figure 7 Generalised circuit structure for a parallel comparison of 2^{m-1} pairs of images

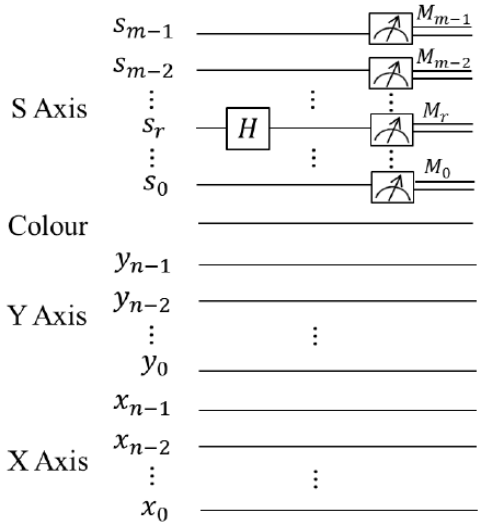

Applying the Hadamard gate that maps the basis state $|0\rangle$ to $(|0\rangle + |1\rangle)/\sqrt{2}$ and $|1\rangle$ to $(|0\rangle - |1\rangle)/\sqrt{2}$ as mentioned in Section 3.2, on the strip wire s_r (expressed by $H_r|S(m, n)\rangle$) transforms the state of the strip into:

$$
\begin{aligned}
H_r\left|S(m,n)\right\rangle &= \frac{1}{2^{m/2}}\sum_{s=0}^{2^m-1}\left|I_s(n)\right\rangle\otimes\left|s_{m-1},\cdots,s_{r+1}\right\rangle \\
&\otimes H\left|s_r\right\rangle\otimes\left|s_{r-1},\cdots,s_0\right\rangle \\
&= \frac{1}{2^{m/2}}\sum_{z=1}^{2^{m-r-1}}\sum_{k=g(z)}^{\frac{1}{2}g(2z)-1}\left|I_k(n)\right\rangle \\
&\otimes\left|s_{m-1},\cdots,s_{r+1}\right\rangle\otimes H\left|0\right\rangle\otimes\left|s_{r-1},\cdots,s_0\right\rangle \\
&+\frac{1}{2^{m/2}}\sum_{z=1}^{2^{m-r-1}}\sum_{k=g(z)}^{\frac{1}{2}g(2z)-1}\left|I_{k+2^r}(n)\right\rangle\otimes\left|s_{m-1},\cdots,s_{r+1}\right\rangle \\
&\otimes H\left|1\right\rangle\otimes\left|s_{r-1},\cdots,s_0\right\rangle \\
&= \frac{1}{2^{(m+1)/2}}\sum_{z=1}^{2^{m-r-1}}\sum_{k=g(z)}^{\frac{1}{2}g(2z)-1}\left(\left|I_k(n)\right\rangle+\left|I_{k+2^r}(n)\right\rangle\right) \\
&\otimes\left|s_{m-1},\cdots,s_{r+1},0,s_{r-1},\cdots,s_0\right\rangle \\
&+\frac{1}{2^{(m+1)/2}}\sum_{z=1}^{2^{m-r-1}}\sum_{k=g(z)}^{\frac{1}{2}g(2z)-1}\left(\left|I_k(n)\right\rangle-\left|I_{k+2^r}(n)\right\rangle\right) \\
&\otimes\left|s_{m-1},\cdots,s_{r+1},1,s_{r-1},\cdots,s_0\right\rangle
\end{aligned}
\tag{24}
$$

where

$$
\begin{aligned}
&\left|I_k(n)\right\rangle\pm\left|I_{k+2^r}(n)\right\rangle = \frac{1}{2^n}\sum_{i=0}^{2^{2n}-1}\left(\left|c_{k,i}\right\rangle\pm\left|c_{k+2^r,i}\right\rangle\right)\otimes\left|i\right\rangle \\
&= \frac{1}{2^n}\sum_{i=0}^{2^{2n}-1}\Big[\left(\cos\theta_{k,i}\pm\cos\theta_{k+2^r,i}\right)\left|0\right\rangle \\
&\qquad +\left(\sin\theta_{k,i}\pm\sin\theta_{k+2^r,i}\right)\left|1\right\rangle\Big]\left|i\right\rangle,
\end{aligned}
\tag{25}
$$

The probability of the readouts from the m measurements are given by

$$
\begin{aligned}
&P_{s_r}\left(\left|s_{m-1},\cdots,s_{r+1},0,s_{r-1},\cdots,s_0\right\rangle\right) \\
&= \frac{1}{2^{m+2n}}\sum_{z=1}^{2^{m-r-1}}\sum_{k=g(z)}^{\frac{1}{2}g(2z)-1}\sum_{i=0}^{2^{2n}-1}1+\cos\left(\theta_k-\theta_{k+2^r}\right) \\
&= \frac{1}{2}+\frac{1}{2^{m+2n}}\sum_{z=1}^{2^{m-r-1}}\sum_{k=g(z)}^{\frac{1}{2}g(2z)-1}\sum_{i=0}^{2^{2n}-1}\cos\sigma_{k,k+2^r}^{i}.
\end{aligned}
\tag{26}
$$

In the same way, that of state $|s_{m-1}, \cdots, s_{r+1}, 1, s_{r-1}, \cdots, s_0\rangle$ on s_r is given by

$$
\begin{aligned}
&P_{s_r}\left(\left|s_{m-1},\cdots,s_{r+1},1,s_{r-1},\cdots,s_0\right\rangle\right)=\frac{1}{2} \\
&-\frac{1}{2^{m+2n}}\sum_{z=1}^{2^{m-r-1}}\sum_{k=g(z)}^{\frac{1}{2}g(2z)-1}\sum_{i=0}^{2^{2n}-1}\cos\sigma_{k,k+2^r}^{i}.
\end{aligned}
\tag{27}
$$

From this, it becomes evident that

$$
\begin{aligned}
&P_{s_r}\left(\left|s_{m-1},\cdots s_{r+1},0,s_{r-1},\cdots,s_0\right\rangle\right) \\
&+P_{s_r}\left(\left|s_{m-1},\cdots,s_{r+1},1,s_{r-1},\cdots,s_0\right\rangle\right)=1.
\end{aligned}
\tag{28}
$$

The states $|s_{m-1}, \cdots, s_{r+1}, 0, s_{r-1}, \cdots, s_0\rangle$ and $|s_{m-1}, \cdots, s_{r+1}, 1, s_{r-1}, \cdots, s_0\rangle$represent all the images that are at the k^{th} and $(k + 2^r)^{\text{th}}$ position of the strip, respectively. In order to determine the similarity of every pair of images, the generalised representation of the probability of $|I_{k+2^r}(n)\rangle$ in the strip is given by

$$
\begin{aligned}
P_{s_r}\left(\left|k+2^r\right\rangle\right) &= \frac{1}{2^{m+2n}}\sum_{i=0}^{2^{2n}-1}1-\cos\left(\theta_k-\theta_{k+2^r}\right) \\
&= \frac{1}{2^m}-\frac{1}{2^{m+2n}}\sum_{i=0}^{2^{2n}-1}\cos\sigma_{k,k+2^r}^{i},
\end{aligned}
\tag{29}
$$

In addition, the similarity between $|I_k(n)\rangle$ and $|I_{k+2^r}(n)\rangle$ can be presented as

$$
\begin{aligned}
sim\left(\left|I_k\right\rangle,\left|I_{k+2^r}\right\rangle\right) &= 1-2^m P_{s_r}\left(\left|k+2^r\right\rangle\right) \\
&= \frac{1}{2^{2n}}\sum_{i=0}^{2^{2n}-1}\cos\sigma_{k,k+2^r}^{i},
\end{aligned}
\tag{30}
$$

where $|I_k\rangle$ and $|I_{k+2^r}\rangle$ are the two images being compared in the strip, $P_{s_r}(|k+2^r\rangle)$ is defined in (29), and $sim(|I_k\rangle, |I_{k+2^r}\rangle) \in [0, 1]$. The similarity between $|I_k(n)\rangle$ and $|I_{k+2^r}(n)\rangle$ which are encoded in the strip comprising 2^m images is also determined in accordance with Definition 3, where

$$
f\left(\sigma_{k,t}^{0},\sigma_{k,t}^{1},\cdots,\sigma_{k,t}^{2^{2n}-1}\right)=\sum_{i=0}^{2^{2n}-1}\cos\sigma_{k,k+2^r}^{i}.
$$

Two examples to demonstrate how two pairs of images can be compared and the implication of applying the Hadamard gate on different strip wires s_0 or s_1 are presented in Figure 8. A strip comprising of four images $|I_0\rangle$, $|I_1\rangle$, $|I_2\rangle$, and $|I_3\rangle$ with the differences between their content captured by their varying colour angles is presented on the left in Figure 8. On the right of the same figure, the circuit in Figure 8(a) is used to compare $|I_0\rangle$ with $|I_1\rangle$ and $|I_2\rangle$ with $|I_3\rangle$ by applying a Hadamard gate on the strip wire s_0, while the circuit in Figure 8(b) is served to compare $|I_0\rangle$ with $|I_2\rangle$ and $|I_1\rangle$ with $|I_3\rangle$ by applying a Hadamard gate on the strip wire s_1.

Figure 8 An example to realise the simultaneous comparison of two pairs of images

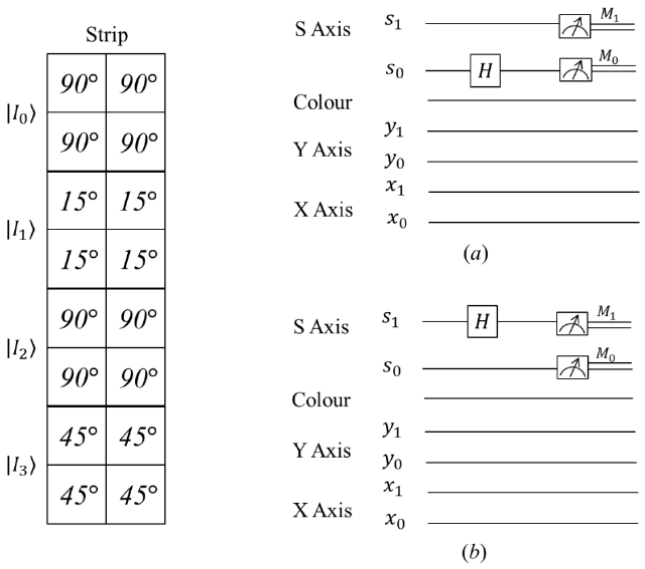

Table 1 Image comparison by applying Hadamard operation on different strip wires

Image comparison	*Circuit*	*Transformed state (Hadamard)*	*Probability*	*Similarity*
$\|I_0\rangle$, $\|I_1\rangle$	Figure 8(a)	$\frac{1}{2\sqrt{2}}\big[(\|I_0\rangle+\|I_1\rangle)\|00\rangle+(\|I_0\rangle-\|I_1\rangle)\|01\rangle$	$P_{s_0}(\|01\rangle)=0.185$	$sim(\|I_0\rangle, \|I_1\rangle)=0.259$
$\|I_2\rangle$, $\|I_3\rangle$		$+(\|I_2\rangle+\|I_3\rangle)\|10\rangle+(\|I_2\rangle-\|I_3\rangle)\|11\rangle$	$P_{s_0}(\|11\rangle)=0.073$	$sim(\|I_2\rangle, \|I_3\rangle)=0.707$
$\|I_0\rangle$, $\|I_2\rangle$	Figure 8(b)	$\frac{1}{2\sqrt{2}}\big[(\|I_0\rangle+\|I_2\rangle)\|00\rangle+(\|I_1\rangle+\|I_3\rangle)\|01\rangle$	$P_{s_1}(\|10\rangle)=0$	$sim(\|I_0\rangle, \|I_2\rangle)=1$
$\|I_1\rangle$, $\|I_3\rangle$		$+(\|I_0\rangle-\|I_2\rangle)\|10\rangle+(\|I_1\rangle-\|I_3\rangle)\|11\rangle$	$P_{s_1}(\|11\rangle)=0.033$	$sim(\|I_1\rangle, \|I_3\rangle)=0.866$

According to (5), the *m*FRQI state of this strip (m = 2, n = 1) is given by

$$|S(2,1)\rangle=\frac{1}{2}\big(|I_0\rangle\otimes|00\rangle+|I_1\rangle\otimes|01\rangle+|I_2\rangle\otimes|10\rangle+|I_3\rangle\otimes|11\rangle\big). \tag{31}$$

The difference between applying the Hadamard gate on strip wire s_0 and s_1 is elaborated in Table 1. The table also shows the transformed state, the probability of the state on strip wires, and the similarity between the images being compared. The probability and similarity are calculated using (29) and (30) where m = 2, n = 1, r = 0 or 1, respectively.

From the discussion in this section and results from the example in Figure 8 as well as Table 1, it is evident that different pairs of images can be compared by simply moving the Hadamard operation from one wire on the S-axis to another. However, comparing some pairs of images such as $|I_0\rangle$ with $|I_3\rangle$, and $|I_1\rangle$ with $|I_2\rangle$ in Figure 8, is difficult to accomplish in this manner because they do not satisfy the relationship defined earlier in (22). Hence, a new strategy is required to deal how to compare two arbitrary images in a strip and is the main focus in Section 3.4.

3.4 Comparison between two arbitrary quantum images and the sub-blocks

As mentioned in Section 3.3, the position of the two images being compared, which are the k^{th} and $(k + 2^r)^{\text{th}}$ images in the strip (r is the index of s_r in the circuit), in a strip is relatively fixed. In order to compare two arbitrary quantum images and/or contents of their sub-blocks from a strip, some geometric transformation and control-conditions are applied to the quantum system. In this section, the more complicated cases of quantum image comparison are discussed such as comparing arbitrary pairs of images, and comparing sub-blocks from two images in a strip. The circuit structure for realising such processes is presented in Figure 9.

The input of this circuit is the *m*FRQI state as defined in (22) (expressed by $|S_I\rangle$ in the circuit), the operation G_S that is applied on the strip wires is the geometric operation which can swap two images in the strip when two arbitrary images are supposed to be compared. A notation '◑' to indicate for '0' or '1' control-condition is adopted throughout the discussion. The additional control-conditions on either of the position axis (Y-axis or X-axis) are necessary in order to confine this Hadamard operation to the required sub-blocks from the images that are being compared. The operation G_I is needed when the sub-blocks being compared are at different positions from the two images. The state in the circuit after applying the Hadamard gate on the r^{th} strip wire is transformed into $H_r G_S \,|\, S_{G_I}\rangle$ as shown in Figure 9.

The similarity between the sub-blocks from two FRQI quantum images encoded in a strip is

$$sim\big(|i_k\rangle, |i_{t\to k+2^r}\rangle\big)=1-2^m\frac{p}{q}P_{s_r}\big(|k+2^r\rangle\big), \tag{32}$$

where $|i_k\rangle$ and $|\, I_{t\to k+2^r}\rangle$ are the sub-blocks from the two images $|I_k\rangle$ and $|\, I_{t\to k+2^r}\rangle$ in the strip, $|\, I_{t\to k+2^r}\rangle$ is the image from the position t to $k + 2^r$ using the geometric transformation on the strip wires, p is the area of the image $|I_k\rangle$ or $|\, I_{t\to k+2^r}\rangle$, and q is the area of the sub-block $|i_k\rangle$ or $|\, i_{t\to k+2^r}\rangle$ in the two images, $P_{s_r}(|\, k+2^r\rangle)$ is the probability of the readouts in the measurements from the state $|k + 2^r\rangle$ as discussed in (29), $sim(|\, i_k\rangle, |\, i_{t\to k+2^r}\rangle)\in[0,1]$.

Figure 9 Generalised circuit structure for parallel comparison of FRQI quantum images

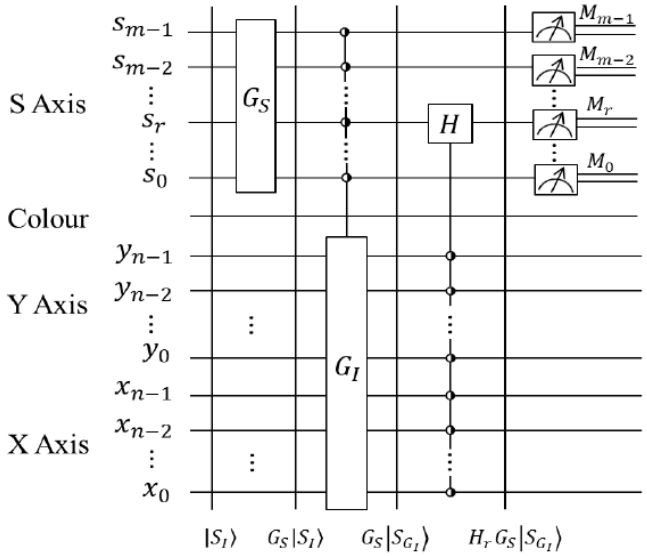

The procedure to determine the similarity of images in a strip in parallel has already been elaborated in Section 3.3. Here, only an example in Figure 10 suffices to illustrate the comparison between two sub-blocks from two arbitrarily located FRQI quantum images.

Figure 10 Comparison of two sub-blocks, ‘C’ and ‘M’ from images $|I_0\rangle$ and $|I_3\rangle$ in strip $|\varphi_0\rangle$

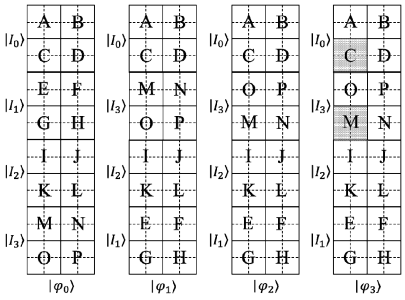

(a)

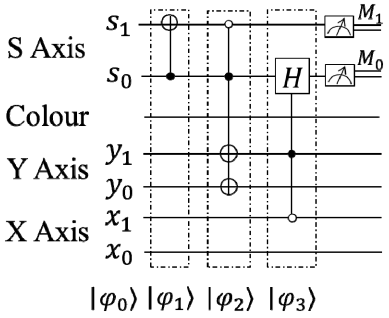

(b)

Note: Strip $|\varphi_1\rangle$, $|\varphi_2\rangle$, and $|\varphi_3\rangle$ in (a) are the midterm states when applying the circuit in (b).

The sub-block ‘C’ from $|I_0\rangle$ is compared with sub-block ‘M’ from $|I_3\rangle$ in $|\varphi_0\rangle$. The midterm states and the corresponding circuit are also presented in the figure. The procedure to accomplish this comparison is:

$|\varphi_0\rangle$ The original strip comprising four quantum images.

$|\varphi_1\rangle$ Swap the position between $|I_1\rangle$ and $|I_3\rangle$ using the C-NOT gate on the strip wires.

$|\varphi_2\rangle$ Flip the position of ‘M’ with ‘O’, ‘N’ with ‘P’ in $|I_3\rangle$ along the X-axis.

$|\varphi_3\rangle$ Compare the two sub-blocks ‘C’ and ‘M’ through applying the Hadamard gate on s_0.

As explained in Figure 8 in Section 3.3, another way to realise the comparison between the sub-blocs ‘C’ and ‘M’ is by first swapping the images $|I_2\rangle$ and $|I_3\rangle$, then flipping the position of sub-block ‘M’ with ‘O’, ‘N’ with ‘P’ in $|I_3\rangle$ along X-axis. Finally, the sub-blocks ‘C’ and ‘M’ are compared by applying the Hadamard gate on s_1.

4 Simulation experiments to assess the similarity of quantum images

In the absence of the physical quantum hardware to implement the image comparison, a conventional desktop computer with Intel Core i7, 2 Duo 2.80 GHz CPU, 4 GB RAM and 64 bit operating system is used to simulate the experiments. The simulation is based on linear algebra with complex vectors as quantum states and unitary matrices as unitary transforms using MATLAB, and the programme is realised by means of equations as well as the definitions which were introduced in the preceding sections. The final step is that of measurement which converts the quantum information to the classical form as probability distributions. Extracting and analysing the distributions gives information for comparing quantum images.

4.1 Comparison of two synthetic quantum images

The first experiment is that to compare two 8 × 8 synthetic images and two 256 × 256 synthetic images both having four grey levels, comprising of black, dark, light, and white colours respectively, as shown on the left in Figure 11 and Figure 12. The purpose of this experiment is to analyse the relationship between the similarity of two images and the size of them.

The comparison between the two 8 × 8 images is executed using the circuit on the right side in Figure 11. The circuit comprises of 8 qubits of which 6 qubits are used to address location of the content of the image, 1 qubit stores the colour information, and the remaining 1 qubit represents the strip wire where the Hadamard and measurement operations are performed. Using the definition in (21), a similarity of 0.31 is obtained for these two images. On the other hand, the similarity value between the two 256 × 256 images, whose circuit consists of 17 wires as shown on the right in Figure 12, is 0.25. The information retrieved from comparing these two sets of images are summarised in Table 2. These results indicate that the similarity between two quantum images increases with increase in the size of the images. As shown in Figure 11 and Figure 12, the operation to compare two images is realised by using only a single Hadamard gate. Accomplishing such a task on a classical computer requires that the colour of every position in the image be compared one at a time. Hence, the proposed method offers a significant speed-up compared to how it is performed using classical computing resources.

Table 2 Summary of comparison results for synthetic images in Figures 11 and 12

Image comparison	*No. of qubits (wires)*	*Probability*	*Similarity*
$\|I_0(3)\rangle$, $\|I_1(3)\rangle$	8	$P_{s_0}(\|1\rangle) = 0.343$	$sim(\|I_0\rangle, \|I_1\rangle) = 0.314$
$\|I_0(8)\rangle$, $\|I_1(8)\rangle$	18	$P_{s_0}(\|1\rangle) = 0.374$	$sim(\|I_0\rangle, \|I_1\rangle) = 0.253$

Figure 11 Two synthetic 8 × 8 FRQI images and the circuit structure for their comparison (see online version for colours)

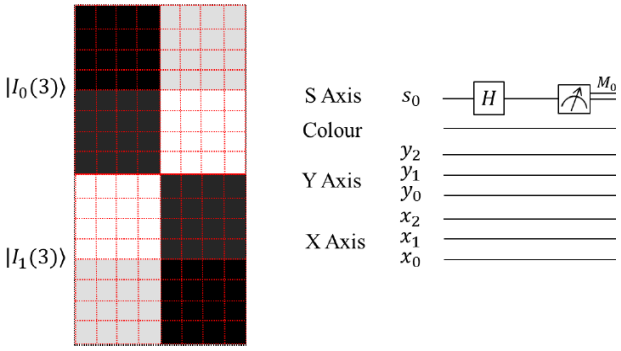

Figure 12 Two synthetic 256 × 256 FRQI images and the circuit structure for their comparison (see online version for colours)

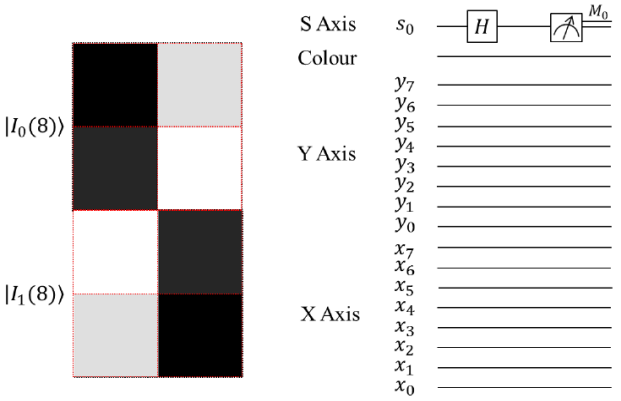

4.2 Parallel comparison of four quantum images in a strip

In the second experiment, a dataset consisting of four 512 × 512 images comprising of the blonde lady, dark-haired lady, bridge, and plane is considered. These images are prepared as $|I_0\rangle$, $|I_1\rangle$, $|I_2\rangle$, and $|I_3\rangle$, respectively and combined to form a strip. For brevity, we represent the strip with only labels of these images as seen on the left in Figure 13. The aim of this experiment is to simultaneously compare $|I_0\rangle$ with $|I_1\rangle$, and $|I_2\rangle$ with $|I_3\rangle$.

Similar to the circuit in Figure 8(a), the circuit to simultaneously compare these two pairs of images is presented in Figure 14. The probabilities of getting the readouts (in *log* scale) on the strip wires in the measurements are presented in Figure 15. The similarities between different pairs of images being compared are shown in the Table 3, all of which suggest $|I_0\rangle$ and $|I_1\rangle$ are more similar to each other than $|I_2\rangle$ and $|I_3\rangle$. A simulation of a single Hadamard gate and two measurement operations are used to obtain the similarities for these two pairs of images. This further demonstrates the low computational requirements of the proposed method in comparison with performing the same task on traditional computing devices.

Figure 13 The strip on the left and the images being compared in the strip

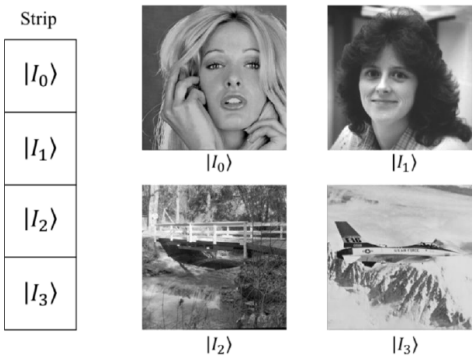

Figure 14 Circuit structure of comparing the images in Figure 13

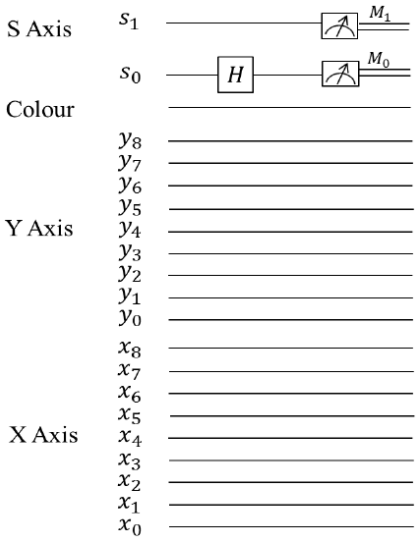

Table 3 Comparison results for the images encoded in the strip in Figure 13

Image comparison	*Probability*	*Similarity*
$\|I_0\rangle$, $\|I_1\rangle$	$P_{s_0}(\|01\rangle) = 0.029$	$sim(\|I_0\rangle, \|I_1\rangle) = 0.883$
$\|I_2\rangle$, $\|I_3\rangle$	$P_{s_0}(\|11\rangle) = 0.040$	$sim(\|I_2\rangle, \|I_3\rangle) = 0.839$

Figure 15 Histogram of the probabilities of the readouts in the measurements

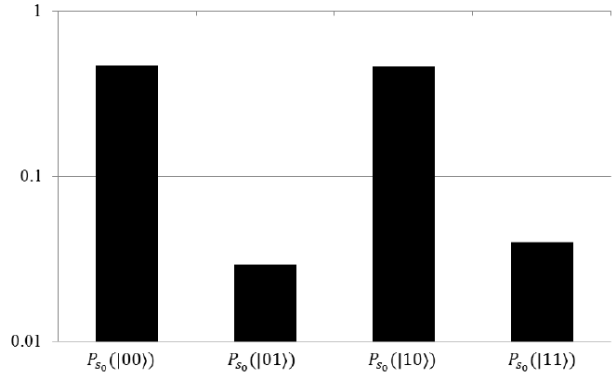

4.3 Comparison of sub-blocks from two FRQI quantum images

The aim of the last experiment is to realise the comparison between two sub-blocks from two arbitrary images in a strip. As shown in Figure 16, we intend to compare the Lena image in the bottom left of the image in $|I_0\rangle$ (labelled as $|i_0^3\rangle$) with the watermarked Lena image in the top right of the image in $|I_3\rangle$ (labelled as $|i_3^2\rangle$), and the man image (labelled as $|i_1^3\rangle$) with the processed man image (labelled as $|i_2^3\rangle$) at the same position in $|I_1\rangle$ and $|I_2\rangle$, respectively. The enlarged versions of these four images that are being compared are presented in the bottom row of the Figure 16. For brevity, the four 1,024 × 1,024 images are indicated by only their labels $|I_0\rangle$, $|I_1\rangle$, $|I_2\rangle$, and $|I_3\rangle$ in the strip on the left in the same figure.

The corresponding circuit structure to compare them is presented in Figure 17. There are four steps to accomplish this comparison:

Step 1 Swap the position between $|I_1\rangle$ and $|I_3\rangle$ using the C-NOT gate on the strip wires.

Step 2 Swap the position of the watermarked Lena image with baboon in $|I_3\rangle$.

Step 3 Compare the two Lena images and two 'man' images in parallel by applying the Hadamard gate on s_0 with appropriate control-condition operations to confine the operation to the desired sub-blocks.

Step 4 Observe the readouts from the quantum measurements to build up a histogram which can reflect the similarity of the two pairs of images.

As discussed in Figure 10 in Section 3.4, another way to execute the same comparison is applying Hadamard gate on strip wire s_1 after swapping the position of $|I_2\rangle$ and $|I_3\rangle$ in the strip.

The probabilities of getting the readouts (in *log* scale) on the strip wires in the measurements are presented in Figure 18, and the similarities among different pairs of images being compared are shown in the Table 4, from which the similarity between the original Lena image and the watermarked Lena image is 0.936. Moreover, the watermarking and authentication of quantum images (Iliyasu et al., 2012a, 2012b) introduced how to realise the watermarked quantum image, however, the use of the peak-signal-to-noise-ratio (PSNR) as an evaluation metric for the fidelity between the original image and the watermarked image needs to be reconsidered in order to atone for the presence of errors in the preparation of the quantum image as well as the procedure to encode and decode the images. Using the proposed comparison scheme, a more accurate comparison can be made between the original quantum image and its watermarked version.

Table 4 Comparison results for the sub-blocks from two images

Image comparison	*Probability*	*Similarity*
$\|i_0^3\rangle, \|i_3^2\rangle$	$P_{s_0}(\|01\rangle) = 0.004$	$sim(\|i_0\rangle, \|i_3\rangle) = 0.936$
$\|i_1^3\rangle, \|i_2^3\rangle$	$P_{s_0}(\|11\rangle) = 0.013$	$sim(\|i_1\rangle, \|i_2\rangle) = 0.787$

The results as indicated in this section show that the comparison of quantum images is both feasible and practical. Therefore, the proposed method provides the foundation for quantum image database search, which is one of the next steps in FRQI quantum image processing.

Figure 16 Parallel comparison of two Lena images and two men images

Figure 17 Circuit structure for realising the comparison in Figure 16

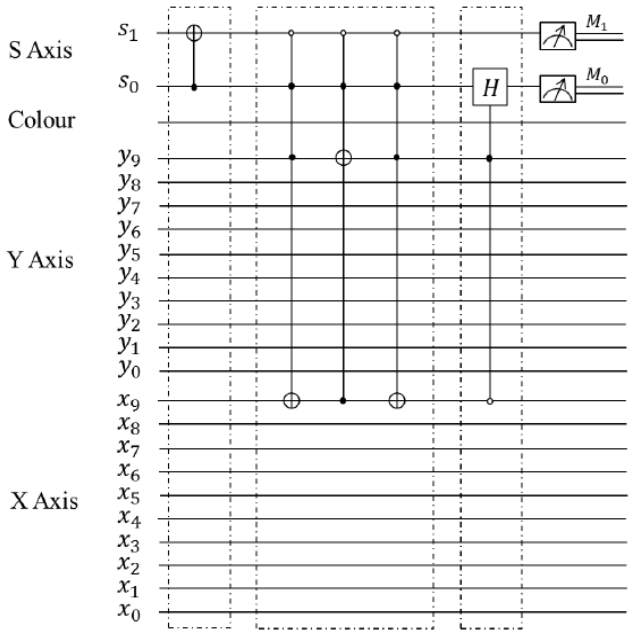

Figure 18 Histogram of the probabilities of the readouts in the measurements

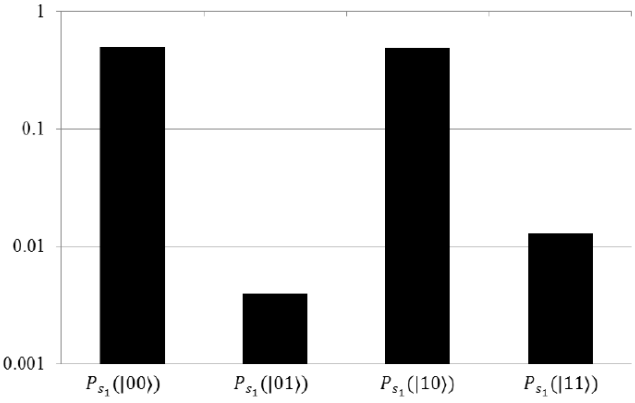

5 Conclusions

A method to evaluate the similarity between FRQI quantum images of equal size is proposed. According to the representation of the strip, which combined by 2^m (m qubits) quantum images being compared and the basic operations in the quantum computation, a similarity value is estimated on the basis of the probability distributions of the readouts from quantum measurements. The proposed method was proven to require less computational resources, and hence, offers a significant speed-up in comparison to performing the same task on traditional computing devices. This is possible because only a single Hadamard gate as well as several control-conditions (when the sub-blocks are compared) is required to simultaneously transform the entire information encoding the quantum images in a strip.

Three simulation-based experiments were implemented using MATLAB on a classical computer by means of linear algebra with complex vectors as quantum states and unitary matrices as unitary transformations provide a reasonable estimation to the image comparison. Parallel comparison of quantum images is executed by constituting the new quantum system with the additional wires (strip). By utilising appropriate geometric transformation operations on the strip wires as well as the required control conditions to the position wires, the comparison between two arbitrary FRQI quantum images in the strip and the comparison between the sub-blocks from two different images can be realised. As a consequence, the work presented has shown that the similarity between two quantum images depends on the entire information in the both images instead of some parts of them, and furthermore, it is related to the size of the two images.

As for future work, the results in this paper will be extended in the following directions. Firstly, the comparison between two quantum images in this paper is based on the cosine function of pixel difference at every position of the images. Quantum Fourier transform (Cleve and Watrous, 2000) or wavelet transform (Fijany and Williams, 1999) could also be applied on FRQI quantum images in order to create different function so as to finish the quantum image comparison. Secondly, the proposal offers a first step towards image database search on quantum computers whereby an image could be retrieved as a search result from a database based on the extent of its similarity in comparison with the particular reference image. To realise such a search procedure, a reconstitution of the quantum system by adding some additional wires to the circuit in order to represent the images in the database and the reference images together might be necessary. Then the comparison is performed between the images to get the best result as the image with highest similarity value to the reference image. Exploiting the parallelism inherent to quantum computation, it is envisaged that quantum image database search will be significantly faster than those on classical computers. Thirdly, besides the ability to measure the difference between the original image and the watermarked image which was suggested earlier, the proposed comparison method presented in this paper can also be applied to the quantum movie (Iliyasu et al., 2011) in order to enhance the smoothness and continuity of the frame to frame transition between scenes, and also to make the quantum movie trailers. These extensions will open new directions for efficient image and video processing using quantum computing hardware.

Acknowledgements

The authors would like to acknowledge the professional suggestions and advices received from distinguished reviewers and members of the *IJICA* editorial team. The work is sponsored by the Japanese Government via the Monbukagakusho scholarship programme.

References

Barenco, A., Bennett, C.H., Cleve, R., et al. (1995) 'Elementary gates for quantum computation', *Phys. Rev. A*, Vol. 52, No. 5, pp.3457–3467.

Beach, G., Lomont, C. and Cohen, C. (2003) 'Quantum image processing (QuIP)', *Proceedings of the 32nd Applied Imagery Pattern Recognition Workshop*, pp.39–44.

Broadbent, A. and Kashefi, E. (2009) 'Parallelizing quantum circuits', *Theoretical Comp. Science*, Vol. 410, No. 26, pp.2489–2510.

Caraiman, S. and Manta, V.I. (2009) 'New applications of quantum algorithm to computer graphics: the quantum random sample consensus algorithm', *Proceedings of the 6th ACM Conference on Computing Frontiers*.

Childs, A.M., Leung, D.W. and Nielsen, M.A. (2005) 'Unified derivations of measurement-based schemes for quantum computation', *Phys. Rev. A*, Vol. 71, No. 3, pp.1–14.

Chow, J.M., Corcoles, A.D. and Gambetta, J.M. (2012) 'High-fidelity gates towards a scalable super-conducting quantum processor', *American Phys. Soc*., Vol. 57, No. 1, P29.00005.

Cleve, R. and Watrous, J. (2000) 'Fast parallel circuits for the quantum Fourier transform', *Proceedings of 41st Annual Symposium on Foundations of Computer Science*, pp.526–536.

Fijany, A. and Williams, C. P. (1999) 'Quantum wavelet transforms: fast algorithms and complete circuits', *Springer LNCS*, Vol. 1509, pp.10–33.

Grover, L. (1996) 'A fast quantum mechanical algorithm for database search', *Proc. 28th Ann. ACM Symp. on Theory of Comput*., pp.212–219.

Iliyasu, A.M., Le, P.Q., Dong, F. and Hirota, K. (2011) 'A framework for representing and producing movies on quantum computers', *Intl. J. of Quantum Info*., Vol. 9, No. 6, pp.1459–1497.

Iliyasu, A.M., Le, P.Q., Dong, F. and Hirota, K. (2012a) 'Watermarking and authentication of quantum images based on restricted geometric transformations', *Info. Sci*., Vol. 186, No. 1, pp.126–149.

Iliyasu, A.M., Le, P.Q., Yan, F., Sun, B., Garcia, J.A., Dong, F. and Hirota, K. (2012b) 'A two-tier scheme for greyscale quantum image watermarking and recovery', *Int'l. J. of Innovative Comp. & Appl*., Vol. 4, No. 3, pp.1–17.

Latorre, J.I. (2005) 'Image compression and entanglement', arXiv: quant-ph/0510031.

Le, P.Q., Dong, F. and Hirota, K. (2010a) 'A flexible representation of quantum images for polynomial preparation, image compression, and processing operations', *Quantum Info. Proc*., Vol. 10, No. 1, pp.63–84.

Le, P.Q., Iliyasu, A.M., Dong, F. and Hirota, K. (2010b) 'Fast geometric transformations on quantum images', *IAENG Intl. J. of Applied Mathematics*, Vol. 40, No. 3, pp.113–123.

Le, P.Q., Iliyasu, A.M., Dong, F. and Hirota, K. (2011a) 'Efficient colour transformations on quantum image', *J. of Adv. Comp. Intl. Info*., Vol. 15, No. 6, pp.698–706.

Le, P.Q., Iliyasu, A.M., Dong, F. and Hirota, K. (2011b) 'Strategies for designing geometric transformations on quantum images', *Theoretical Comp. Science*, Vol. 412, No. 15, pp.1406–1418.

Le, P.Q., Iliyasu, A.M., Dong, F. and Hirota, K. (2011c) 'A flexible representation and invertible transformations for images on quantum computers', *New Advances in Intelligent Signal Processing, Book Series: Studies in Computational Intelligence*, Vol. 372, pp.179–202, Springer-Verlag.

Moore, C. and Nilsson, M. (2001) 'Parallel quantum computation and quantum codes', *SIAM Journal on Computing*, Vol. 31, No. 3, pp.799–815.

Nagy, M. and Akl, S.G. (2006) 'Quantum computation and quantum information', *Intl. J. of Parallel, Emergent and Distributed Systems*, Vol. 21, No. 1, pp.1–59.

Nielsen, M. and Chuang, I. (2000) *Quantum Computation and Quantum Information*, Cambridge University Press, New York.

Shor, P.W. (1994) 'Algorithms for quantum computation: discrete logarithms and factoring', *Proc. 35th Ann. Symp. Found. Comput. Sci*., pp.124–134.

Venegas-Andraca, S.E. and Bose, S. (2003) 'Storing, processing and retrieving an image using quantum mechanics', *Proc. SPIE Conf. Quantum Info. and Comput*., Vol. 5105, pp.134–147.

Yan, F., Le, P.Q., Iliyasu, A.M., Sun, B., Garcia, J.A., Dong, F. and Hirota, K. (2012) 'Assessing the similarity of quantum images based on probability measurements', *2012 IEEE World Congress on Computational Intelligence*, pp.1–6.